Macromolecules

Article

Supramolecular Assembly via Noncovalent Metal Coordination Chemistry: Synthesis, Characterization, and Elastic Properties

Christina Ott, Johannes M. Kranenburg, Carlos Guerrero-Sanchez, Stephanie Hoeppener, Daan Wouters, and Ulrich S. Schubert

Macromolecules, **2009**, 42 (6), 2177-2183• DOI: 10.1021/ma802298p • Publication Date (Web): 20 February 2009

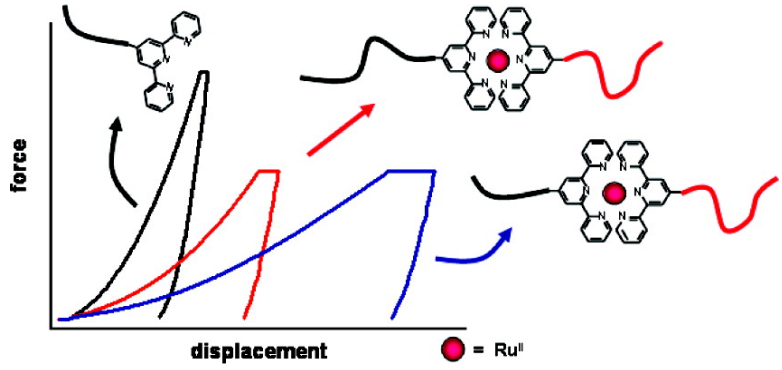

More About This Article

Additional resources and features associated with this article are available within the HTML version:

- Supporting Information
- Access to high resolution figures
- Links to articles and content related to this article
- Copyright permission to reproduce figures and/or text from this article

View the Full Text HTML

Supramolecular Assembly via Noncovalent Metal Coordination Chemistry: Synthesis, Characterization, and Elastic Properties

Christina Ott,[†] Johannes M. Kranenburg,[†,‡] Carlos Guerrero-Sanchez,[†,‡] Stephanie Hoeppener,[†] Daan Wouters,[†] and Ulrich S. Schubert*[,†,‡,§]

Laboratory of Macromolecular Chemistry and Nanoscience, Eindhoven University of Technology, P.O. Box 513, 5600 MB Eindhoven, The Netherlands; Dutch Polymer Institute (DPI), P.O. Box 902, 5600 AX Eindhoven, The Netherlands; and Laboratory of Organic and Macromolecular Chemistry, Friedrich-Schiller-University Jena, Humboldtstr. 10, 07743 Jena, Germany

Received October 13, 2008; Revised Manuscript Received January 15, 2009

ABSTRACT: Terpyridine-functionalized alternating 1,1-diphenylethylenene (DPE)/styrene copolymers with different chain lengths were used to form metallo-supramolecular block copolymers with hydrophilic poly(ethylene glycol) blocks. In this contribution, the synthesis of new A-[Ru]-B and A-[Ru]-B-[Ru]-A block copolymers is described. The investigation of the mechanical properties and thermal transitions of these materials revealed that the AB block copolymers with different A block length span a large stiffness range. Further characterization includes nuclear magnetic resonance spectroscopy, gel permeation chromatography, and ultraviolet−visible spectroscopy which proved the purity of the materials. Moreover, the formation of micellar aggregates of the amphiphilic block copolymers in water was studied by transmission electron microscopy.

Introduction

The development of novel functional materials with advanced and improved properties represents an important research topic in the field of material science and polymer technology. Supramolecular chemistry plays an essential role since reversible noncovalent interactions, such as metal coordination, hydrogen bonding, van der Waals forces, $\pi-\pi$ interactions, and electrostatic effects, provide access to highly ordered structures using bottom-up approaches generated by spontaneous self-assembly.[1] This research area is inspired by biological systems, which use these weak noncovalent interactions to a great extent. The incorporation of supramolecular moieties into polymers is considered to be an attractive method for the engineering of new functional materials.[2,3]

The extraordinary versatility of this approach relies on the easy tuning of bond strength, lifetime, and directionality by applying external stimuli such as temperature, pH value, redox state, and shear forces.[4] Tethering chelating ligands[5−10] (e.g., bipyridines or terpyridines) to macromolecules or polymers allows the formation of metal complexes in the presence of suitable transition metal ions. Most commonly used metal ions for terpyridine systems are, e.g., Fe, Ru, Os, Co, Ni, Pt, Cu, Mn, Ag, Zn, Cd, and Hg in low oxidation states which form pseudo-octahedral complexes with two terpyridine ligands upon complexation.[11] Os and Ru ions are of special importance since no ligand exchange takes place. Therefore, they are referred to as inert metal−terpyridine complexes. This approach allows the synthesis of heteroleptic bis-terpyridine complexes[12,13] and hence the formation of metallo-supramolecular block copolymers when different polymer chains are linked to each other. Therefore, supramolecular chemistry can be regarded as an alternative to well-known polymerization techniques, such as living anionic polymerization[14−16] or controlled radical polymerization[17−21] (e.g., ATRP, NMRP, RAFT), which represent established techniques for the preparation of covalently bonded block copolymers featuring controlled architectures and compositions. The powerful strategy of combining controlled/living polymerization techniques with supramolecular chemistry allows the synthesis of hybrid materials using the supramolecular complexation approach, generating complex systems from simpler building blocks in a kind of LEGO procedure.[22] In this way, a virtually unlimited amount of new (multifunctional) materials with specific photochemical, electrochemical, and photophysical properties[23−25] can be created in a straightforward fashion. Further fine-tuning of the materials' properties on a molecular and nanoscale level allows the application in various technological fields.

The combination of two thermodynamically incompatible segments within the same material gives rise to wide range of nanostructures in bulk[26] and in solution.[27−29] The chemical link between the different segments prevents phase separation at the macroscopic length scale; however, regular structures can be designed with periodicities of the phases in the nanometer region. Depending on the composition of the block copolymers and the interactions between the blocks different morphologies can be adjusted, whereby the nanostructures contribute to the physical and chemical properties of the material. Such systems are employed in (industrial) applications ranging from high-impact plastics, thermoplastic elastomers, additives, and foams as well as drug delivery systems and information storage.[30]

In this contribution, we report the synthesis of new (mechanical) property improved metallo-supramolecular A-[Ru]-B and A-[Ru]-B-[Ru]-A block copolymers. For this purpose, an alternating diphenylethylene/styrene copolymer functionalized with terpyridine moieties provided the basis for the complexation reaction. Amphiphilic block copolymers were obtained by reacting the terpyridine-functionalized copolymer with a poly(ethylene glycol) ruthenium(III) monocomplex. Polymers containing diphenylethylene reveal improved long-term service temperatures due to the stiffening of the polymer main chain by the bulky phenyl rings.[31] Therefore, they are often referred to as "superpolystyrene" (SPS). The PEG chains are representing a relatively soft component; thus, the influence of the microphase separation on the mechanical properties was investigated using depth-sensing indentation. Thermal transitions of the obtained supramolecular A-[Ru]-B materials were analyzed by DSC and compared to those of the starting materials.

* Corresponding author: e-mail u.s.schubert@tue.nl; fax +(31)-402474186.
† Eindhoven University of Technology.
‡ Dutch Polymer Institute.
§ Friedrich-Schiller-University Jena.

10.1021/ma802298p CCC: $40.75
Published on Web 02/20/2009

Scheme 1. Schematic Representation of the Reaction for the Synthesis of the Amphiphilic Block Copolymers Consisting of an Alternating Diphenylethylene/Styrene Copolymer and a Poly(ethylene glycol) Block

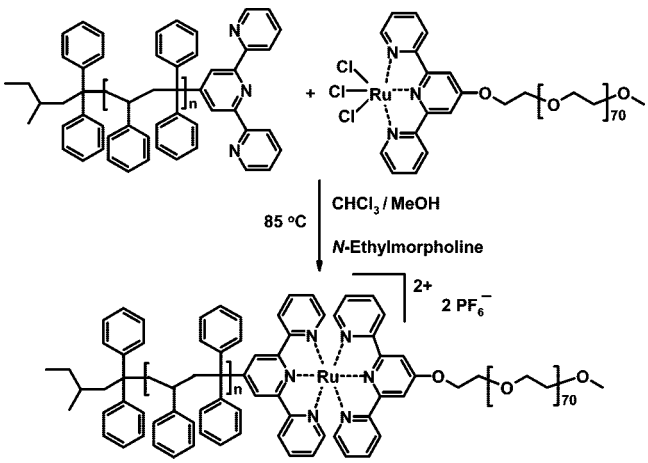

Experimental Section

Synthesis of the Terpyridine-Functionalized Diphenylethylene/Styrene Copolymers (SPS_n-[). Anionic polymerizations were carried out in a 100 mL round-bottom Schlenk-type glass flask using inert atmosphere techniques. All utilized glassware were previously heated above 150 °C, subjected to several cycles of subsequent filling with argon and high vacuum, and kept under argon prior to use. A predetermined amount of 1,1-diphenylethylene was added into the Schlenk flask containing a predetermined amount of cyclohexane at 55 °C under an argon atmosphere. After the addition of *sec*-butyllithium, the mixture turned into a deep red solution. In the final step, styrene was added to the mixture, which was stirred for 1.5 h. The functionalization started with the addition of a predetermined volume (1.25 molar excess with respect to *sec*-butyllithium) of a solution of 4′-chloro-2,2′:6′,2″-terpyridine in toluene into the Schlenk flask at room temperature. Finally, methanol was added after 8 h in order to terminate the reaction. The polymers were precipitated from chloroform into methanol. The obtained materials were dried at 40 °C under vacuum for 24 h. ^{1}H NMR (SPS_{11}-[, 400 MHz, CD_2Cl_2): δ = 8.63 (m, 2 H; $H_{6:6'}$), 8.54 (m, 2 H; $H_{3:3''}$), 8.16 (m, 2 H; $H_{3':5'}$), 7.84 (m, 2 H; $H_{4:4''}$), 7.45−6.95 (m, 177 H; $H_{\text{aromatic DPE \& styrene}}$, $H_{5:5''}$), 2.50−0.00 (m, 66 H; $H_{\text{aliphatic polymer backbone, }C_4H_9\ sec\text{-butyl group}}$).

Synthesis of the SPS_n-[Ru]-PEG_{70} Block Copolymers. The terpyridine-functionalized styrene/diphenylethylene copolymer (90 mg, M_n = 2200 g/mol) and the $RuCl_3$ poly(ethylene oxide) monocomplex[32] (157 mg, M_n = 3200 g/mol) were reacted in a 1:1.2 molar ratio in a 3:1 (1.5 mL/0.5 mL) solvent mixture of degassed chloroform and methanol for 6 h at 85 °C in a sealed vial. Subsequently, the reaction mixture was stirred for 10 min at room temperature after a 10-fold excess of NH_4PF_6 was added. The solution was poured into water, and the aqueous layer was extracted twice with chloroform. The combined organic layers were dried over Na_2SO_4, filtered, and evaporated in vacuo. The crude product was purified by preparative size exclusion chromatography (Biobeads SX1) and column chromatography (AlOx).

The following metallo-supramolecular block copolymers have been synthesized using the previous described procedure: SPS_{11}-[Ru]-PEG_{70}, SPS_{22}-[Ru]-PEG_{70}, SPS_{39}-[Ru]-PEG_{70}, and SPS_{66}-[Ru]-PEG_{70}. ^{1}H NMR (SPS_6-[Ru]-PEG_{70}, 400 MHz, CD_2Cl_2): δ = 8.45−8.26 (m, 8 H; $H_{3':5''}$, $H_{3:3''}$), 8.16−7.94 (m, 4 H; $H_{4:4''}$), 7.93−7.77 (m, 4 H; $H_{6:6''}$), 7.70−5.95 (m, 104 H; $H_{\text{PS,DPE backbone aromatic}}$; H_{aromatic}, $H_{5:5''}$), 4.09 (m, 2 H; tpyOCH_2), 3.88−3.36 (m, 280 H; $H_{\text{PEG backbone}}$), 2.40−0.10 (m, 41 H; $H_{\text{PS \& DPE backbone aliphatic, }sec\text{-butyl group}}$).

Synthesis of the $RuCl_3$ SPS Monocomplexes. A 3-fold excess of anhydrous $RuCl_3$ (85 mg, M = 207 g/mol) with respect to the terpyridine end-functionalized polymer was heated in dry degassed DMA (3 mL) to 130 °C. After the color of the suspension turned brown, a solution of the terpyridine-functionalized SPS (300 mg, M_n = 2200 g/mol) in dry degassed DMA (2 mL) was added dropwise. Stirring was continued overnight at 130 °C at inert conditions, and then the solution was allowed to cool to room temperature. The resulting mixture was partitioned between dichloromethane and water. The organic layer was separated, dried over Na_2SO_4, filtered, and evaporated in vacuo. The brown residue was dissolved in a minimum amount of THF and precipitated twice into methanol. ^{1}H NMR ($CDCl_3$): Only the polymer backbone was visible because of the paramagnetic nature of Ru(III) complex.

Synthesis of the SPS_n-[Ru]-PEG_{44}-[Ru]-SPS_n Block Copolymers. Bis(terpyridine) end-functionalized poly(ethylene oxide)[33] (30 mg, M_n = 2500 g/mol) and $RuCl_3$ poly(S-*alt*-DPE) monocomplex (63 mg, M_n = 2400 g/mol) were reacted in a 1:2.2 molar ratio in a 3:1 (1.2 mL/0.4 mL) solvent mixture of degassed chloroform and methanol for 6 h at 85 °C in a sealed vial. The purification was performed analogue to the SPS_n-[Ru]-PEG_{70} block copolymers.

The following metallo-supramolecular block copolymers have been synthesized using the previously described procedure: SPS_6-[Ru]-PEG_{44}-[Ru]-SPS_6 and SPS_{11}-[Ru]-PEG_{44}-[Ru]-SPS_{11}. ^{1}H NMR (SPS_6-[Ru]-PEG_{44}-[Ru]-SPS_6, 400 MHz, CD_2Cl_2): δ = 8.45−8.26 (m, 16 H; $H_{3':5''}$, $H_{3:3''}$), 8.16−7.94 (m, 8 H; $H_{4:4''}$), 7.93−7.77 (m, 8 H; $H_{6:6''}$), 7.70−5.95 (m, 118 H; $H_{\text{PS,DPE backbone aromatic}}$; H_{aromatic}, $H_{5:5''}$), 4.09 (m, 4 H; tpyOCH_2), 3.88−3.36 (m, 176 H; $H_{\text{PEG backbone}}$), 2.40−0.10 (m, 82 H; $H_{\text{PS \& DPE backbone aliphatic, }sec\text{-butyl group}}$).

Characterization of the Copolymer Systems. GPC measurements were performed either on a Shimadzu system with a SCL-10A system controller, a LC-10AD pump, a RID-6A refractive index detector, and a Polymer Laboratories PLgel 5 μm Mixed-D column using *N,N*-dimethylacetamide (DMA) as eluent at a flow rate of 1 mL/min (M_n values were calculated against polystyrene standards) or on a Waters system with a 1515 pump, a 2414 refractive index detector, and a Waters Styragel HT4 column utilizing a *N,N*-dimethylformamide (DMF) and 5 mM NH_4PF_6 solution as eluent at a flow rate of 0.5 mL/min at 50 °C (M_n values were calculated against poly(ethylene glycol) standards). ^{1}H NMR spectra were recorded on a Varian Gemini 400 spectrometer using deuterated methylene chloride (Cambridge Isotopes Laboratories) at room temperature. UV−vis spectra were recorded on a Perkin-Elmer Lambda 45P spectrophotometer using quartz cuvettes (1 cm path length). Transmission microscopy measurements were performed on a FEI Tecnai 20, type Sphera TEM operating at 200 kV with a LaB_6 filament and a bottom mounted 1k × 1k Gatan CCD. Samples were prepared by blotting a dilute solution of the respective micelle solution on a 200 mesh carbon-coated grid followed by overnight drying, after which the grids were examined in the TEM. TEM grids were hydrophilized directly before use by 40 s plasma treatment. The samples for TEM measurements were not stained. Thermal transitions were determined on a NETSCH 204 F1 Phoenix DCS in a nitrogen atmosphere. Samples were two times heated from −50 to 225 °C at a rate of 20 K min^{-1}. The first heating run was disregarded. Polymer films were prepared for depth-sensing indentation by drop-casting the materials onto glass slides (Marienfeld, Lauda-Königshofen, Germany). The solutions contained 5 mg of polymer in 50 μL of chloroform (Biosolve). Several commercial polystyrenes, Styron 678 and Styron 648 (DOW Chemical) as well as N5000 (Shell), were drop-cast from toluene and dried thoroughly. The elastic properties of the dried samples were studied at 11% relative humidity by depth-sensing indentation (DSI) using a Hysitron (Minneapolis, MN) TriboIndenter equipped with a Berkovich (trigonal pyramid) probe. During the indentation experiments, the tip was loaded to maximum load in 10 s, held at maximum load for 10 s, and unloaded in 0.5 s. For each material, the experiments were repeated on at least two different drop-casted samples and at least five maximum loads (1500, 1200, 900, 600, and 300 μN). For SPS_{11}-[Ru]-PEG_{70}, lower loads were chosen: 300, 250, 200, 150, 100, 50 μN. Multiple indentation experiments were performed on SPS_n-[employing maximum loads of 400, 1000, and 1600 μN. The polystyrenes were measured employing maximum

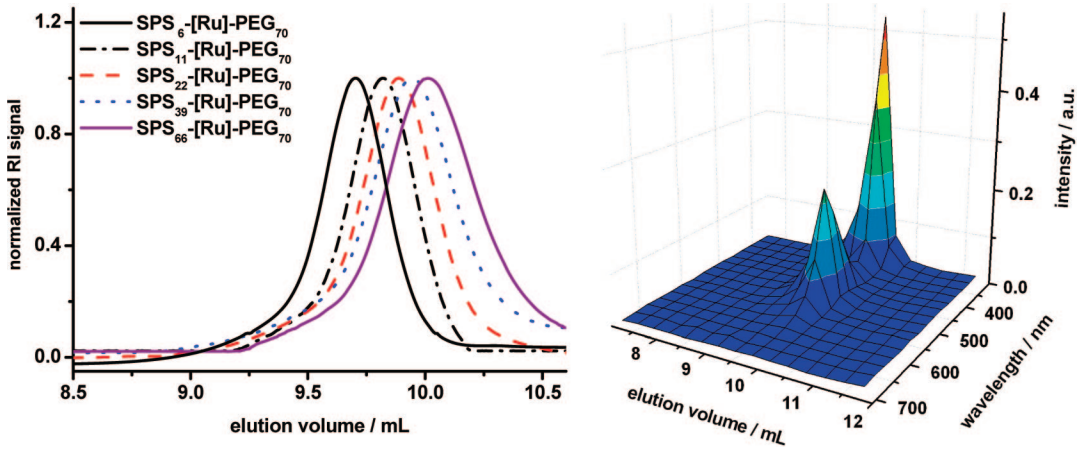

Figure 1. GPC curves of the purified metallo-supramolecular block copolymers (left) and one example for the combination of GPC with a PDA detector (SPS_{22}-[Ru]-PEG_{70}).

loads of 2700, 2400, 2100, 1800, 1500, and 1200 μN, and indentation experiments were repeated on SPS_n-[at these loads as well. The first two indentation responses were left out to minimize the effect of thermal drift. The load−displacement responses obtained from DSI were analyzed using the method proposed by Oliver and Pharr.[34,35] Reduced moduli E_r were converted to modulus of elasticity E_i (where the subscript denotes "indentation") using 0.35 as the Poisson's ratio.[36]

Preparation of the Micelles. The block copolymers were dissolved in tetrahydrofuran (THF) at a concentration of 1 g L^{-1}. Subsequently, drops of water were added stepwise to induce aggregation of the insoluble SPS block. After that an equal amount of water was added in one shot to "freeze" the micelles.

Results and Discussion

We described very recently the synthesis of terpyridine-functionalized alternating diphenylethylene/styrene copolymers via anionic polymerization.[37] In order to form heteroleptic complexes with ruthenium, i.e., for metallo-supramolecular block copolymers, a two-step synthesis is required. In the first step, one of the terpyridine-substituted compounds, here terpyridine-functionalized poly(ethylene glycol), is reacted with ruthenium(III) chloride to obtain the corresponding ruthenium(III) monocomplex. Subsequently, the monocomplex is reduced to Ru(II) in the presence of a reducing agent, and the chlorides are replaced by an uncoordinated second terpyridine ligand.[12,38] The synthetic approach of the bis-complex formation is depicted in Scheme 1. Evidence for the purity of the polymer was obtained by GPC. Even though charged supramolecular polymers, such as bis(terpyridine)ruthenium(II) complexes, interact strongly with the column material, addition of 5 mM NH_4PF_6 to the GPC eluent (*N,N*-dimethylformamide) minimizes this effect.[39] Since metallo-supramolecular polymers show a characteristic absorption in the visible region (at around 490 nm), the GPC measurements were also performed using a photodiode-array detector providing an UV−vis spectrum for every retention time. This provides additional information over the purity of the material. Figure 1 displays the GPC spectra (RI detector) of five ruthenium-containing block copolymers which consist of varying styrene/diphenylethylene block lengths as well as an example for the 3-dimensional GPC spectrum using the photodiode-array detector which reveals the characteristic absorption band for ruthenium bis-terpyridine complexes at around 490 nm for all retention times of the polymer. ^{1}H NMR spectroscopy provided an additional indication for the successful complex formation. The terpyridine protons in 6,6″- and in the 3′,5′- position are influenced by the coordination of the two ligands in a meridional fashion, resulting in a significant shift of their resonances. Table 1 summarizes the molar masses and the polydispersity indices of the starting materials and the corresponding block copolymers obtained by ^{1}H NMR spectroscopy and GPC.

Table 1. M_n Values, Polydispersity Indices (PDI), and Glass Transition Temperatures (T_g) of the Uncomplexed Copolymers and the Corresponding Metallo-supramolecular Block Copolymers

polymer	$M_{n,NMR}$ (g/mol)	$M_{n,GPC}$ (g/mol) PDI	T_g (°C)
SPS_{11}-[	3600	2100 (1.17)[a]	137
SPS_{22}-[	6700	4700 (1.11)[a]	156
SPS_{39}-[	11600	7800 (1.14)[a]	164
SPS_{66}-[	19200	10800 (1.21)[a]	160
SPS_{11}-[Ru]-PEG_{70}	7200	5700 (1.05)[b]	n.d.
SPS_{22}-[Ru]-PEG_{70}	9900	5200 (1.11)[b]	126
SPS_{39}-[Ru]-PEG_{70}	15200	4700 (1.12)[b]	138
SPS_{66}-[Ru]-PEG_{70}	22800	4400 (1.08)[b]	142

[a] GPC in DMA with LiCl (2.1 g/L) as eluent using polystyrene calibration. [b] GPC in DMF with NH_4PF_6 (0.8 g/L) as eluent using poly(ethylene glycol) calibration.

In addition to the metallo-supramolecular diblock copolymers, A-[Ru]-B-[Ru]-A triblock copolymers were synthesized where block A corresponds to the alternating styrene/diphenylethylene copolymer and block B to the midsegment poly(ethylene glycol). Scheme 2 demonstrates the synthetic approach for this reaction. Commercially available hydroxy-functionalized poly(ethylene glycol) was postfunctionalized with terpyridine units using a suspension of potassium hydroxide and 4-chloro-2,2′:6,2″-terpyridine in DMSO at 70 °C to yield the corresponding terpyridine-terminated poly(ethylene glycol).[40,41] The terpyridine-functionalized alternating copolymer was reacted with $RuCl_3$ and converted into the corresponding Ru(III) monocomplex. The isolated polymer complex revealed the characteristic MLCT-band for monocomplexes at ∼400 nm in the UV−vis spectrum. ^{1}H NMR spectroscopy revealed no terpyridine signals in the region between 9 and 7 ppm due to the paramagnetic nature of the complex proving the formation of the desired complexes. Subsequently, the polymer complex was utilized as an end-capper in the reaction with the terpyridine-functionalized poly(ethylene glycol) to obtain the A-[Ru]-B-[Ru]-A triblock copolymers. Figure 2 displays the GPC spectrum of the purified SPS_6-[Ru]-PEG_{44}-[Ru]-SPS_6 block copolymer recorded with a photodiode array detector.

As a result of the above-described reactions, the hydrophilic poly(ethylene glycol) block is chemically tethered to the hydrophobic block using noncovalent coordination interactions. The combination of thermodynamically incompatible blocks within the same material may lead to phase separation. In

Scheme 2. Schematic Representation of the Synthesis of Ruthenium-Containing Triblock Copolymers

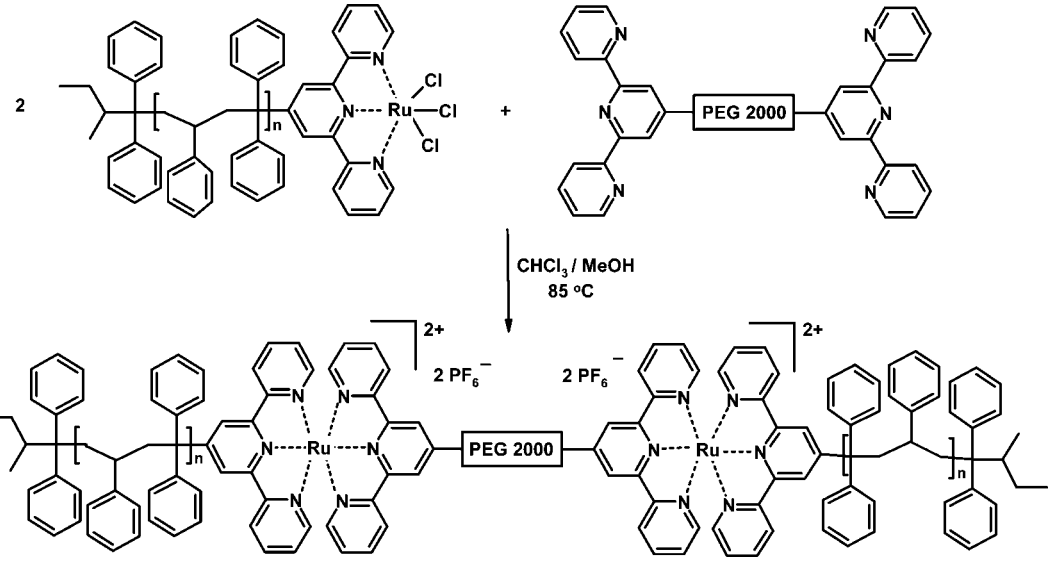

addition, amphiphilic block copolymeters can form polymeric micelles in solution via association into nanoscopic core/shell structures. In the present study, this was investigated by transmission electron microscopy (TEM) for the A-[Ru]-B materials based on PEG_{70}. For this purpose, the A-[Ru]-B block copolymers were dissolved in a minimum amount of THF. Subsequently, the selective solvent (H_2O) was added dropwise, leading to the formation of the polymeric micelles. Afterward, the common solvent (THF) was removed by dialysis against deionized water. Micelles with a rather uniform diameter of 19−27 nm were observed. For TEM imaging, no contrast agent was necessary to visualize the spherical micelles due to the presence of ruthenium in the polymers. Figure 3 represents an example for the formed spherical micelles in water of SPS_{39}-[Ru]-PEG_{70}, demonstrating the different solubility of the PEG and SPS blocks. In these TEM pictures, the SPS core of the micelles corresponds basically to the micelle sizes shown in the image since the PEG coronal chains are expected to collapse on the core during the drying process. The micelles related to the largest sample (SPS_{66}-[Ru]-PEG_{70}) are of comparable size as the micelles of SPS_{39}-[Ru]-PEG_{70}. Indeed, it has been recently demonstrated that the size of the core of PS-[Ru]-PEG micelles did not scale with the 3/5 power of the degree of polymerization (DP) of the PS block as usually observed for "covalent" PS-*b*-PEG micelles. In fact, the micellar core size was observed to be constant for the DP of the PS block lower than 200. This effect was explained by the presence of the charged and bulky bis-terpyridine ruthenium(II) complexes (-[Ru]-) at the interface of the PS and PEG blocks that affected the micellar core size to a certain value.[42] However, no stable micelles could be observed by TEM for the block copolymers consisting of a short hydrophobic block (SPS_{11}-[Ru]-PEG_{70} and smaller). In those cases, the core of the micelle collapsed upon evaporation of the solvent, and a polymer film of uniform thickness was formed on the TEM grid.

For solid materials, the relative block length relates to the volume fraction of the constituents, which is, together with the interaction between the different polymers, expressed in the Flory−Huggins interaction parameter,[26] the governing parameter for phase separation. The volume fraction of the constituents and the extent of phase-separation affect many bulk properties. Therefore, it is possible to tailor the mechanical properties of the SPS-[Ru]-PEG by varying the block sizes or the number of hard/soft blocks within the copolymer.

Thermal transitions were investigated by differential scanning calorimetry (DSC). The glass transition T_g of the terpyridine-functionalized SPS increased from 137 °C for $n = 11$ to 165 °C for $n = 66$ (Figure 4a, Table 1). This is in agreement with the common observation that the T_g is reduced for smaller chain lengths.[43] The SPS chains are expected to be more rigid than polystyrene chains because the extra phenyl ring restricts its free rotation. Indeed, the glass transition temperature of the SPS

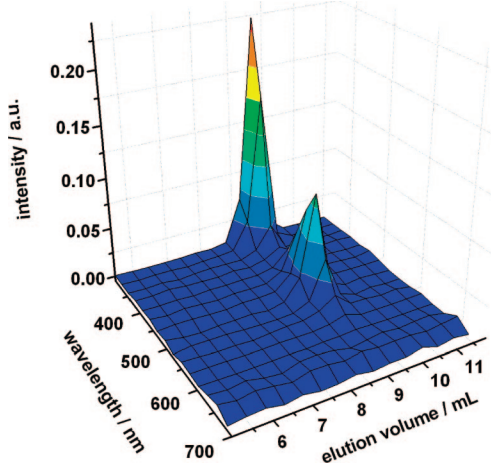

Figure 2. GPC with PDA detector of the SPS_6-[Ru]-PEG_{44}-[Ru]-SPS_6 triblock copolymer.

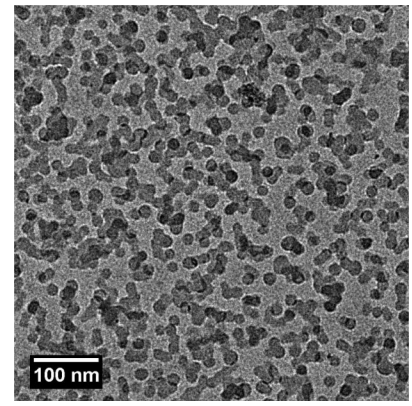

Figure 3. TEM image of the unstained micelles in water of SPS_{39}-[Ru]-PEG_{70}.

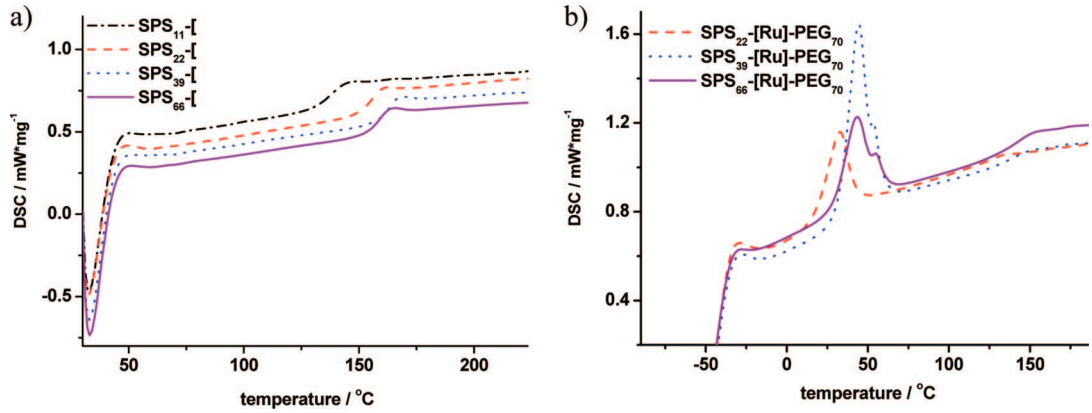

Figure 4. Thermal transitions of (a) the alternating terpyridine-functionalized copolymers and (b) the complexed block copolymers, as measured by DSC.

was higher than for polystyrene: the T_g of conventional polystyrene of corresponding molar mass increases from 55 to 89 °C and reaches at higher molar mass a plateau value of 100 °C.[44,45] The SPS$_n$-[Ru]-PEG$_{70}$ block copolymers show a decreased T_g compared to the corresponding SPS$_n$-[counterparts: due to the softer poly(ethylene glycol) PEG present in or around the SPS-rich phase, the chains in this phase obtain segmental mobility already at lower temperatures (Table 1). Moreover, the melting peak of poly(ethylene glycol) at around 50 °C is clearly visible in the DSC graph (Figure 4b). Also, the SPS$_{11}$-[Ru]-PEG$_{44}$-[showed a comparable melting point (at ∼55 °C, data not shown).[46]

One of the key mechanical properties for materials is the elastic modulus or Young's modulus. In order to study the elastic behavior of the SPS-[and the SPS-[Ru]-PEG materials, depth-sensing indentation (DSI) experiments were conducted. In spite of the gentle drying procedure after dropcasting, several supramolecular materials exhibited extensive cracking due to the volume change upon drying. One of the advantages of DSI is that spots where the film adhered to the substrate could be easily identified (from the absence of fringes in the optical image of the film), and indentation experiments could be successfully performed exactly on those spots. Only on the SPS$_{66}$-[Ru]-PEG$_{70}$ samples, no suitable spots were found. Cracks in the films indicate brittleness of the material. For very brittle materials cracking may occur also on the smaller scale during the indentation experiment. In that case, the method employed to analyze the indentation load−displacement responses is not valid.[34] Therefore, for selected materials, the surface was imaged with the indenter tip after performing the indentation experiments. However, no fracture was observed at the corners of the indents or around the indents.

The indentation modulus of SPS$_n$-[was 5.91 GPa with a standard deviation of 0.27 GPa (average and standard deviation obtained by treating all indents on SPS$_n$-[as one data set). The indentation modulus of SPS$_n$-[decreased to a very minor extent with increasing degree of polymerization, from 6.00 ± 0.27 GPa for $n = 11$ to 5.74 ± 0.18 GPa for $n = 66$. This small decrease, which is less than one standard deviation, might be caused by a tiny amount of solvent that remained trapped for the SPS with higher degree of polymerization n but could be removed from the studied SPS samples with lower n. The absence of a clear dependency on the degree of polymerization also indicates that the effect of the terpyridine end group on the materials stiffness can be neglected. We measured an E_i of 4.2 GPa for the commercial polystyrenes (indentation moduli for Styron 678, Styron 648, and N5000 were very close to each other), which corresponds well with indentation moduli of polystyrene reported in the literature for indents to maximum indentation

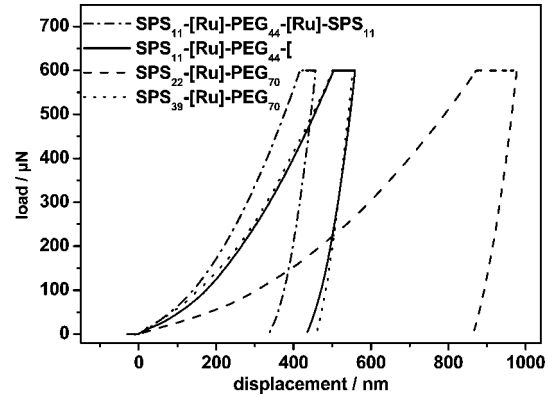

Figure 5. Indentation load−displacement responses for selected supramolecular block copolymers.

depths of 0.5−0.7 μm.[36] (For polymers, the indentation modulus E_i exceeds the Young's elastic modulus E due to some material pile-up at the indent perimeter, nonlinear viscoelasticity, and some other factors.[35,47]) Gausepohl et al.[31] observed a Young's modulus of 4.2 GPa for SPS compared to 3.2 GPa for polystyrene. We note the good agreement between the ratio of the stiffnesses reported by Gausepohl, $E_{PS}/E_{SPS} = 0.76$, and the ratio discussed in the current work, $E_{i,PS}/E_{i,SPS} = 0.71 \pm 0.03$.

The elastic behavior of the obtained supramolecular A-[Ru]-B block copolymers was also investigated. Figure 5 shows that, upon loading to the same load, the displacement of the indenter probe into the surface of SPS$_{22}$-[Ru]-PEG$_{70}$ is larger than into SPS$_{39}$-[Ru]-PEG$_{70}$, reflecting its softer character. In Figure 6, the obtained indentation moduli are presented as a function of SPS content. This measure for the SPS content is calculated by dividing the mass of the SPS by the sum of the masses of the SPS, terpyridine moieties, (counter)ions, and PEG. It is noted that the stiffness is usually modeled as a function of the volume fraction of the constituting phases and not on the weight fractions of the components.[48] Considering that the density of SPS, which is necessary to calculate the SPS volume fraction, is unknown and that at least for some of the materials the phases consist of a mixture of PEG and SPS, weight fractions are plotted in Figure 6. With increasing weight fraction of the hard-domain forming block, i.e., with increasing length of the SPS blocks, the stiffness of the A-[Ru]-B block copolymer increases (filled circles in Figure 6). We note that with increasing length of the SPS block the weight fraction of the metal−ligand complex (MLC) and the PF_6 counterions decreases (annotated numbers in Figure 6). These may influence the stiffness of the material, for instance through electrostatic interactions or by influencing the phase behavior of the material.[49,50]

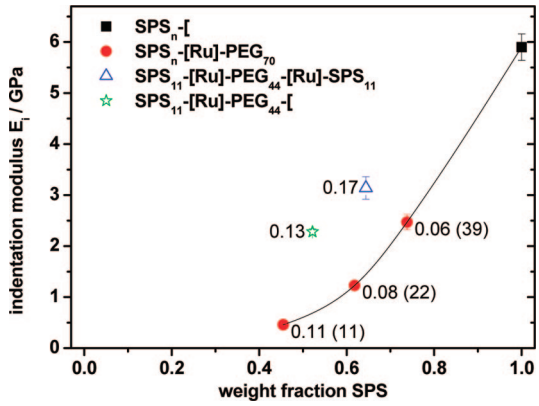

Figure 6. Stiffness of the SPS and the supramolecular block copolymers as a function of the SPS weight fraction. The counterion and metal−ligand complex weight fraction is annotated to the data. For the SPS$_n$-[Ru]-PEG$_{70}$, the degree of polymerization is added in brackets.

Poly(ethylene glycol) is semicrystalline and, depending on the crystallinity, hygroscopic. This implies that the elastic properties of the PEG-containing materials may be affected by their processing history as well as by the humidity. To check the humidity influence on the stiffness of the supramolecular copolymers, the indentation measurements were repeated at 45% relative humidity. For apolar polymers such as polystyrene and SPS, the humidity did not have any effect on the load−displacement responses and thus also not on the modulus. The investigated A-[Ru]-B materials containing the hygroscopic PEG block did not show any significant decrease in modulus upon repeating the experiments at ambient humidity either. Therefore, it can be concluded that the humidity can be neglected in these cases.

Figures 5 and 6 also show the load−displacement responses and indentation moduli for SPS$_{11}$-[Ru]-PEG$_{44}$-[and SPS$_{11}$-[Ru]-PEG$_{44}$-[Ru]-SPS$_{11}$. These materials exhibited a higher stiffness than the A-[Ru]-B block copolymers of comparable SPS content synthesized with monofunctionalized PEG$_{70}$ (filled circles in Figure 6). The moduli can also be plotted as a function of the total "stiff moiety content" (defined as the weight fraction of the SPS, terpyridine moieties, Ru ions, and counterions). In general, this equals right-shifting of the data by the value annotated in Figure 6 (see Supporting Information). Then the stiffness of the SPS$_{11}$-[Ru]-PEG$_{44}$-[Ru]-SPS$_{11}$ material is comparable to that of a A-[Ru]-B block copolymer of similar stiff moiety content synthesized with monofunctionalized PEG$_{70}$. However, the SPS$_{11}$-[Ru]-PEG$_{44}$-[still is located above the trendline constituted by the SPS-[Ru]-PEG$_{70}$ materials. The higher stiffness for the materials containing the shorter PEG is attributed to their higher Ru^{2+} and PF_6^- ion contents. Small-angle X-ray scattering above the melting point of the PEG showed for PS$_{20}$-[Ru]-PEG$_{70}$ that the MLC and the PF_6^- counterions form randomly located domains surrounded by a mixed PEG/PS phase.[49] For the PEG$_{44}$ materials, the domains containing the MLC and counterions are located closer to each other, and the MLC and counterion weight fraction is higher than for the PEG$_{70}$ materials. Therefore, their effect on the deformation behavior increases. These domains are expected to increase the materials stiffness through electrostatic interaction and/or by impeding the motion of the attached SPS and PEG chain. Furthermore, the presence of the MLC and the counterions may induce changes in the phase-separation behavior of the PEG and SPS as well.[49,50] Also, the smaller size of the PEG may cause differences in phase-separation (and crystallization) behavior compared to the PEG$_{70}$ materials,[26,51] resulting in changes in the relative amounts of the phases present and their thermal transition temperatures, thereby also influencing the materials stiffness.[52]

Conclusion

New AB diblock copolymers and ABA triblock copolymers were successfully synthesized in which the polymer blocks are linked together by a ruthenium(II) complex. Characterization methods that prove the purity of the materials include ^{1}H NMR spectroscopy and GPC, equipped with a photodiode array detector. It was demonstrated that the elastic modulus of supramolecular materials can be changed by varying the chemical composition. In the current work, the chemical composition was fine-tuned by changing the length of the soft-domain and hard-domain forming blocks. The high modulus of SPS, which is ∼35% higher than for PS, provides a wide range for tuning the materials stiffness via this supramolecular approach.

Acknowledgment. The authors thank the Dutch Counsel for Scientific Research (NWO, VICI award for U.S.S.), the Dutch Polymer Institute (DPI), and the Fonds der Chemischen Industrie for financial support.

Supporting Information Available: Stiffness of the supramolecular block copolymers as a function of the stiff moiety content (Figure SI). This material is available free of charge via the Internet at http://pubs.acs.org.

References and Notes

(1) Lehn, J.-M. *Polym. Int.* **2002**, *51*, 825.
(2) Brunsveld, L.; Folmer, B. J. B.; Meijer, E. W.; Sijbesma, R. P. *Chem. Rev.* **2001**, *101*, 4071.
(3) Schubert, U. S.; Eschbaumer, C. *Angew. Chem., Int. Ed.* **2002**, *41*, 2892.
(4) Gosche, A. J.; Steele, I. M.; Ceccarelli, C.; Rheingold, A. L.; Bosnich, B. *Proc. Natl. Acad. Sci. U.S.A.* **2002**, *99*, 4823.
(5) Wu, W.; Collins, J. E.; McAlvin, J. E.; Cutts, R. W.; Fraser, C. L. *Macromolecules* **2001**, *34*, 2812.
(6) Corbin, P. S.; Webb, M. P.; McAlvin, J. E.; Fraser, C. L. *Biomacromolecules* **2001**, *2*, 223.
(7) Marin, V.; Holder, E.; Hoogenboom, R.; Schubert, U. S. *J. Polym. Sci., Part A: Polym. Chem.* **2004**, *42*, 4153.
(8) Eisenbach, C. D.; Schubert, U. S. *Macromolecules* **1993**, *26*, 7372.
(9) Chujo, Y.; Sada, K.; Saegusa, T. *Macromolecules* **1993**, *26*, 6320.
(10) Lohmeijer, B. G. G.; Schubert, U. S. *J. Polym. Sci., Part A: Polym. Chem.* **2004**, *42*, 4016.
(11) Constable, E. C. *Adv. Inorg. Chem. Radiochem.* **1986**, *30*, 69.
(12) Sullivan, B. P.; Calvert, J. M.; Meyer, T. J. *Inorg. Chem.* **1980**, *19*, 1404.
(13) Buckingham, D. A.; Dwyer, F. P.; Sargeson, A. M. *Aust. J. Chem.* **1964**, *17*, 622.
(14) Szwarc, M.; Levy, M.; Milkovich, R. *J. Am. Chem. Soc.* **1956**, *78*, 2656.
(15) Szwarc, M. *Nature (London)* **1956**, *178*, 1168.
(16) Baskaran, D.; Müller, A. H. E. *Prog. Polym. Sci.* **2007**, *32*, 173.
(17) Matyjaszewski, K.; Xia, J. *Chem. Rev.* **2001**, *101*, 2921.
(18) Kamigaito, M.; Ando, T.; Sawamoto, M. *Chem. Rev.* **2001**, *101*, 3689.
(19) Hawker, C. J.; Bosman, A. W.; Harth, E. *Chem. Rev.* **2001**, *101*, 3661.
(20) Fischer, H. *Chem. Rev.* **2001**, *101*, 3581.
(21) Moad, G.; Rizzardo, E.; Thang, S. H. *Polymer* **2008**, *49*, 1079.
(22) Lohmeijer, B. G. G.; Schubert, U. S. *J. Polym. Sci., Part A: Polym. Chem.* **2003**, *41*, 1413.
(23) Islam, A.; Ikeda, N.; Nozaki, K.; Okamoto, Y.; Gholamkhass, B.; Yoshimura, A.; Ohno, T. *Coord. Chem. Rev.* **1998**, *171*, 355.
(24) Stone, M. L.; Crosby, G. A. *Chem. Phys. Lett.* **1981**, *79*, 169.
(25) Schubert, U. S.; Eschbaumer, C.; Andres, P.; Hofmeier, H.; Weidl, C. H.; Herdtweck, E.; Dulkeith, E.; Morteani, A.; Hecker, N. E.; Feldmann, J. *Synth. Met.* **2001**, *121*, 1249.
(26) Bates, F. S.; Fredrickson, G. H. *Phys. Today* **1999**, *52*, 32.
(27) Rodriguez-Hernandez, J.; Chécot, F.; Gnanou, Y.; Lecommandoux, S. *Prog. Polym. Sci.* **2005**, *30*, 691.
(28) Discher, D. E.; Eisenberg, A. *Science* **2002**, *297*, 967.
(29) Riess, G. *Prog. Polym. Sci.* **2003**, *28*, 1107.
(30) Hadjichristidis, N.; Pispas, S.; Floudas, G. A. *Block Copolymers, Synthetic Strategies, Physical Properties, and Applications*; John Wiley & Sons: New York, 2002.

(31) Gausepohl, H.; Oepen, S.; Knoll, K.; Schneider, M.; McKee, G.; Loth, W. *Design. Monomer Polym.* **2000**, *3*, 299.
(32) Ott, C.; Wouters, D.; Thijs, H. M. L.; Schubert, U. S. *J. Inorg. Organomet. Polym. Mater.* **2007**, *17*, 241.
(33) Chiper, M.; Meier, M. A. R.; Kranenburg, J. M.; Schubert, U. S. *Macromol. Chem. Phys.* **2007**, *208*, 679.
(34) Oliver, W. C.; Pharr, G. M. *J. Mater. Res.* **1992**, *7*, 1564.
(35) Kranenburg, J. M.; Tweedie, C. A.; Hoogenboom, R.; Wiesbrock, F.; Thijs, H. M. L.; Hendriks, C. E.; Van Vliet, K. J.; Schubert, U. S. *J. Mater. Chem.* **2007**, *17*, 2713.
(36) Briscoe, B. J.; Fiori, L.; Pelillo, E. *J. Phys., Part D: Appl. Phys* **1998**, *31*, 2395.
(37) Ott, C.; Guerrero-Sanchez, C.; Pavlov, G. M.; Schubert, U. S., submitted.
(38) Reiff, W. M., Jr.; Erickson, N. E. *J. Am. Chem. Soc.* **1968**, *90*, 4794.
(39) Meier, M. A. R.; Lohmeijer, B. G. G.; Schubert, U. S. *Macromol. Rapid Commun.* **2003**, *24*, 852.
(40) Schubert, U. S.; Hien, O.; Eschbaumer, C. *Macromol. Rapid Commun.* **2000**, *21*, 1156.
(41) Schubert, U. S.; Eschbaumer, C. *Macromol. Symp.* **2001**, *163*, 177.
(42) Guillet, P.; Fustin, C.-A.; Lohmeijer, B. G. G.; Schubert, U. S.; Gohy, J.-F. *Macromolecules* **2006**, *39*, 5484.
(43) Young, R. J.; Lovell, P. A. *Introduction to Polymers*, 2nd ed.; Chapman & Hall: London, 1991.
(44) Claudy, P.; Létoffé, J. M.; Camberlain, Y.; Pascault, J. P. *Polym. Bull.* **1983**, *9*, 208.
(45) Brandrup, J.; Immergut, E. H.; Grulke, E. A. *Polymer Handbook*, 4th ed.; John Wiley & Sons: New York, 1999.
(46) It is noted that apart from the crystalline fraction, part of the PEG is expected to be amorphous and above its glass transition at room temperature. Furthermore, the crystallinity observed with DSC is higher than the crystallinity of the samples subjected to indentation: During the DSC experiment (prior to the analyzed traces), the samples were dried at high temperature and subsequently cooled to lower temperatures than the indentation samples. Crystallization of PEG proceeds at a lower temperature than melting [ref 51] and is enhanced by thorough drying.
(47) Tranchida, D.; Piccarolo, S.; Loos, J.; Alexeev, A. *Macromolecules* **2007**, *40*, 1259.
(48) Nielsen, L. E. *Rheol. Acta* **1974**, *13*, 86.
(49) Al-Hussein, M.; de Jeu, W. H.; Lohmeijer, B. G. G.; Schubert, U. S. *Macromolecules* **2003**, *36*, 9281.
(50) Al-Hussein, M.; de Jeu, W. H.; Lohmeijer, B. G. G.; Schubert, U. S. *Macromolecules* **2005**, *38*, 2832.
(51) Zhu, L.; Cheng, S. Z. D.; Calhoun, B. H.; Ge, Q.; Quirk, R. P.; Thomas, E. L.; Hsiao, B. S.; Yeh, F.; Lotz, B. *Polymer* **2001**, *42*, 5829.
(52) For the SPS_{11}-[Ru]-PEG_{44}-[Ru]-SPS_{11} material, an additional reason for the higher stiffness compared to the SPS-[Ru]-PEG may be its different architecture (ABA vs AB). However, this represents probably only a small effect as the hard phase is the continuous phase at these SPS contents [ref 26]; then, additional interactions between the hard phase regions are not as effective in raising the stiffness as for thermoplastic elastomers, where the soft phase is the continuous phase.

MA802298P